https://doi.org/10.5194/hess-2019-305
Preprint. Discussion started: 10 July 2019

Hydrology and Earth System Sciences
Discussions

Weak sensitivity of the terrestrial water budget to global soil texture maps in the ORCHIDEE land surface model

Salma TAFASCA[1], Agnès DUCHARNE[1], Christian VALENTIN[2]

[1] METIS (Milieux Environnementaux, Transferts et Interactions dans les Hydrosystèmes et les Sols), Institut Pierre Simon Laplace (IPSL), Sorbonne Université, CNRS, EPHE, Paris, France

[2] iEES-Paris (Institut d'Ecologie et des Sciences de l'Environnement de Paris), Sorbonne Université, CNRS, INRA, IRD, Paris, France

Correspondence to: Salma Tafasca (salma.tafasca@upmc.fr)

Abstract. Soil physical properties play an important role for estimating soil water and energy fluxes. Many hydrological and land surface models (LSMs) use soil texture maps to infer these properties. Here, we investigate the impact of soil texture on soil water fluxes and storage at global scale using the ORCHIDEE LSM, forced by several complex or globally-uniform soil texture maps. The model shows a realistic sensitivity of runoff processes and soil moisture to soil texture, and reveals that medium textures give the highest evapotranspiration and lowest total runoff rates. The three tested complex soil texture maps being rather similar by construction, especially when upscaled at the 0.5◦ resolution used here, they result in similar water budgets at all scales, compared to the uncertainties of observation-based products and meteorological forcing datasets. A useful outcome is that the choice of the input soil texture map is not crucial for large-scale modelling. The added-value of more detailed soil information (horizontal and vertical resolution, soil composition) deserves further studies.

1. Introduction

Land surface models (LSMs) simulate water and energy fluxes at the interface between the land surface and the atmosphere. They were developed for continental to global scales to provide realistic land boundary conditions to climate models (Remaud et al., 2018), and to investigate the water, energy and carbon cycles at the Earth surface, and the related natural resources and risks (Guimberteau et al., 2017; Haddeland et al., 2011; Sterling et al., 2013; Zhao et al., 2017). By lack of sufficient spatial coverage for detailed soil properties, LSMs, like many physically-based hydrological models, rely on pedotransfer functions (PTF), which relate available soil information to the required soil properties (Looy et al., 2017; De Lannoy et al., 2014). The simplest approach, still used by most LSMs, relies on soil texture, as classified by the US Department of Agriculture (USDA) into 12 soil classes based on the percent of sand, silt and clay particles (USDA Soil Survey Staff et al., 1951). Look-up tables relate these broad texture classes to multiple soil properties, usually with one single central value for each class and property, as found in Cosby et al. (1984) and Carsel and Parrish (1988) for the Clapp and Hornberger (1978) and Van Genuchten (1980) soil water models, respectively.

In this framework, several global soil texture maps are used by LSMs, with different resolutions and soil texture distributions: Zobler (1986) and Reynolds et al. (2000) provided soil texture maps at a resolution of 1° and 5 arc-min

https://doi.org/10.5194/hess-2019-305
Preprint. Discussion started: 10 July 2019

respectively, both based on the 1:5,000,000 FAO/UNESCO Soil Map of the World (FAO/UNESCO, 1971-1981), itself based on soil surveys defining 106 soil units; the latter map was updated as the Harmonized World Soil Database (HSWD), produced at 30 arc-sec by including new regional and national soil information (Nachtergaele et al., 2010; Batjes, 2016); the soil texture map of the 1-km SoilGrids database, although not independent from the above FAO/UNESCO global soil maps, relies on large number of national and international soil profile databases, combined with automated spatial prediction models (Hengl et al., 2014).

Most studies concluding that soil texture exerts an important impact on soil hydrology were conducted at small to medium scales, either through site measurements (e.g. An et al., 2018; Song et al., 2010), or regional-scale and multi-site data analysis (Lehmann et al., 2018; Wang et al., 2009) and model sensitivity analyses. Using a mesoscale hydrologic model over the Mississippi river basin, Livneh et al. (2015) compared two different soil texture maps, and the more spatially detailed one better reproduced hydrologic variability and extreme events. With the Noah LSM over China, Zheng and Yang (2016) found that the sensitivity of the simulated water budget to soil texture was dependent on climate, soil moisture being less sensitive to soil texture in arid areas, while evapotranspiration and runoff showed the highest sensitivity in the transitional zones. Li et al. (2018) confirmed these results over the Tibetan Plateau but showed additional influence of the vegetation cover on the sensitivity to soil texture, as also found over the US (Xia et al., 2015). At a global scale, De Lannoy et al. (2014) developed an improved soil texture map for the Catchment LSM, by merging several texture and organic material maps. Combined with updated PTF, this new map offered modest yet significant improvements of the simulated hydrology compared to various point-scale measurements. Related studies revealed a strong impact of soil water-holding capacity and its spatial patterns using the first generations of LSMs, but with bucket-type soil hydrology instead of Richards equation (Milly & Dunne 1994; Ducharne & Laval, 2000).

Here, we aim at exploring more systematically the impact of soil texture on the water budget at a global scale, using a state-of-the-art LSM with physically-based soil hydrology, and multiple input soil texture maps.

2. Materials and Methods

2.1. Soil texture in the ORCHIDEE LSM

ORCHIDEE (ORganizing Carbon and Hydrology in Dynamic EcosystEms) is the land component of the IPSL (Institut Pierre-Simon Laplace) climate model, and describes the complex links between vegetation phenology and the water, energy and carbon exchanges at the land surface (Krinner et al., 2005). We use here the version of ORCHIDEE developed for CMIP6 (Eyring et al., 2016) and detailed in forthcoming papers (Ducharne et al., in prep), but we deactivated the soil freezing option for simplicity.

The physically-based soil hydrology scheme solves the vertical soil moisture redistribution based on a multi-layer solution of Richards equation, using a 2-m soil discretized into 11 soil layers (de Rosnay et al., 2002), and a special

https://doi.org/10.5194/hess-2019-305
Preprint. Discussion started: 10 July 2019


Hydrology and Earth System Sciences
Discussions

processing for infiltration (d'Orgeval et al., 2008; Vereecken et al., 2019). The unsaturated values of hydraulic conductivity and diffusivity are given by the model of Mualem (1976) - Van Genuchten (1980). In each grid cell, the corresponding parameters (saturated hydraulic conductivity K_s, inverse of air entry suction α, shape parameter m, porosity, and residual moisture) are taken from Carsel and Parrish (1988), as a function of the dominant USDA soil texture class, itself derived from an input soil texture map. To account for the effects soil compaction and bioturbation, K_s decreases exponentially with depth, while the effect of horizontally-variable K_s on infiltration is described by an exponential distribution. Finally, soil texture also influences heat capacity and conductivity (Wang et al., 2016).

Evapotranspiration is described by a classical bulk aerodynamic approach, distinguishing four sub-fluxes: sublimation, interception loss, soil evaporation, and transpiration. The latter two depend on soil moisture and properties, which control how the corresponding rates are reduced compared to the potential rate: transpiration is limited by a stomatal resistance, increasing when soil moisture drops from field capacity to wilting point; soil evaporation is not limited by a resistance, but only by upward capillary fluxes, which control the soil propensity to meet the evaporation demand.

2.2. Simulation protocol

We performed nine global-scale simulations with ORCHIDEE (tag2.0), using different soil texture maps and climatic forcing datasets (Table 1). The analysed period is 1980-2010, following a 20-year warm-up since 1960 to provide accurate initial conditions. Atmospheric forcing datasets being known to exert a first-order influence on LSM results (Guo et al., 2006; Yin et al., 2018), we used two different datasets to drive our simulations, to compare the related uncertainties to the ones coming from the different soil texture maps. Both datasets were constructed at a 0.5° resolution by downscaling and bias-correcting an atmospheric reanalysis. All simulations but one use the GSWP3-v1 meteorological dataset (van den Hurk et al., 2016), with a 3-hourly time step, and based on the 20th Century Reanalysis (20CR; Compo et al., 2011). In contrast, simulation EXP1 uses the 6-hourly CRU-NCEP-v7 meteorological dataset (Wei et al., 2014), based on the NCEP/NCAR reanalysis (Kalnay et al., 1996), and extended beyond 1957-1996 in near real-time.

The three simulations EXP2 to EXP4 rely on complex soil texture maps to define the dominant texture class of each 0.5° grid cell (Figure 1): the 1° map of Zobler (1986) originally contains 5 soil textural classes, but is simplified by ORCHIDEE into three USDA texture classes (Sandy Loam, Loam, and Clay Loam); the 5-arc-min map of Reynolds et al. (2000) uses the USDA classification and is used directly; the SoilGrids map was provided at a 0.5° resolution by the Soil Parameter Model Intercomparison Project (SP-MIP, Gudmundsson & Cuntz, 2017), which aims at quantifying to which degree the differences between LSMs result from soil parameter specification. It was upscaled from the original 1km map of Hengl et al. (2014) by selecting the dominant soil texture in every 0.5° pixel.

In addition, we tested four spatially uniform texture maps, corresponding to the Loam, Loamy Sand, Silt, and Clay classes (EXP6 to EXP9), to assess the effects of medium and extreme soil texture on the global water budget. These simulations were defined by SP-MIP, and rely on hydraulic parameter values given by Schaap et al. (2001) for each USDA

https://doi.org/10.5194/hess-2019-305
Preprint. Discussion started: 10 July 2019

class. We ran an additional simulation (EXP 5) with SoilGrids and the soil parameters of Schaap et al. (2001) to quantify the difference induced by this PTF compared to the default PTF of ORCHIDEE (Carsel & Parrish, 1988) used with SoilGrids in EXP4.

2.3. Calculation of median diameter *dm* for each of the 12 USDA soil texture classes

Every texture class is represented by a polygon in the USDA textural triangle (Fig. 1d). For each texture class, we located the centroid of the corresponding polygon to obtain a central value of the composition in clay, silt and sand particles (Table 2). These clay, silt and sand particles have various diameters, respectively ranging in [0, 2µm], [2µm, 50µm] and [50µm, 2000µm] (USDA; Staff, 1951). To construct the particle-size distribution curve of each texture class (Fig. 2), we further assumed that clay, silt and sand particle diameters are uniformly distributed in the latter intervals. The median diameter of each texture class is then obtained by intersecting the corresponding curve with a cumulative value of 50%, such that half of soil particles reside above this point, and half reside below this point. The resulting median diameters are listed in Table 2. Carsel and Parrish (1988) provide the mean content of sand, silt and clay for each soil texture, but their estimations are based on American soil surveys, which might not be representative of the whole globe, so we preferred to use the composition of the of the polygon centroids. Note that using the mean composition of by Carsel and Parrish (1988) leads to very similar results.

2.4. Evaluation datasets

To assess the realism of our simulations, we use three different datasets. Jung et al. (2010) constructed a series of global 1° evapotranspiration maps at the monthly time step from 1982 to 2008, by interpolating in situ eddy-covariance measurements from the FLUXNET network owing to machine learning algorithms and ancillary geospatial information (land surface remote sensing and meteorology). GLEAM (Martens et al., 2017) is another series of global evapotranspiration maps, provided by at the 0.25° resolution and the daily time step over 1980-2015. They strongly rely on remote-sensing datasets (radiation, precipitation, temperatures, surface soil moisture, vegetation optical depth, snow water equivalents), used as input to an evapotranspiration model based on Priestley and Taylor (1972). Finally, Rodell et al. (2015) quantified the mean annual fluxes of the water cycle at the beginning of the 21st century, at a coarser scale (continents and majors ocean basins) but with the aim of providing consistent estimates of precipitation, evaporation, and runoff, by combining in situ and satellite measurements, data assimilation systems, and multiple energy and water budget closure constraints.

3. Results

3.1. Point scale sensitivity to the 12 USDA texture classes

To check if the ORCHIDEE model displays a realistic response to soil texture, we examined how the pluri-annual means of the main water budget variables relate to soil texture (Fig. 3). We clustered all the points with a similar texture, and sorted

https://doi.org/10.5194/hess-2019-305
Preprint. Discussion started: 10 July 2019

the texture classes based on their median particles diameter (section2.3). The mean fluxes were also divided by mean precipitation to reduce the effect of misleading texture-climate associations, as between sandy classes and arid climates. We focused on EXP2, because the Reynolds map exhibits the largest range of soil textures. Yet, like in the other two complex maps, Loam is by far the most dominant texture (44 %), followed by Sandy Loam, Clay Loam and Sandy Clay Loam (Fig. 1). In EXP2-Reynolds, these four textures alone correspond to 83% of the land surface (Fig. 3a). The texture Silt is absent from the map, and the classes Silty Clay, Silty Clay Loam and Sandy Clay cover only 0.17% of the land surface, so their hydrological response can be severely influenced by other factors than soil texture, explaining their outlier behaviour compared to the other textures for some variables.

The simulated soil moisture, drainage and surface runoff exhibit a clear monotonic response to soil texture (sorted by median diameter). Increasing soil moisture for finer textures is explained by their higher water retention and field capacity. The values of soil parameters for the 12 USDA soil texture classes are detailed in Supplementary S1 and depicted in Figure S1. The opposite responses of drainage and surface runoff (Fig. 3f-g) both result from higher permeability in coarser soils, enhancing drainage and infiltration at the soil surface, thus reducing surface runoff. As it sums up two opposite responses, total runoff shows a larger spread and a non-monotonic (convex) behavior, with smaller total runoff for medium textures.

The opposite response (concave) is found for evapotranspiration (Fig. 3d), because precipitation is partitioned between evapotranspiration and total runoff in every grid cell. The highest evapotranspiration rates found for medium textures is consistent with the high available water capacity for these loamy textures (Fig. S1). Transpiration, however, increases as soil gets coarser (Fig. 3c), and the most likely explanation is that the high conductivity of coarse soils enhances water infiltration at the soil surface, quickly available for plant uptake. Rather surprisingly, we find here that drainage and transpiration decrease when soil moisture gets higher. This indicates that annual mean soil moisture is the result more than the cause of these fluxes, which are strongly driven by hydraulic conductivity when their dependence on mean precipitation is filtered.

Soil evaporation shows more variability within a soil texture class than between the different soil texture classes (Fig. 3b), showing this flux strongly depends on other factors (temperature, leaf area index, etc.). To exclude their spurious effects, we also analysed in Figure 4 the effect of changing soil texture (from EXP2 to EXP4) at the point-scale, thus under similar climatic and land cover conditions. Figure 4 shows the changes occurring when a soil texture class in Reynolds map is replaced by another in SoilGrids map. The Zobler map was excluded from this analysis since it contains only three soil texture classes. Switching maps from Reynolds to SoilGrids (EXP2 to EXP4) results in a majority of land points with unchanged texture, and thus, similar simulated variables. These land points are represented by the diagonal pixels of the matrices and consist of 41.2% of the land surface. Land points with coarser texture in SoilGrids represent 34.1% of the land

https://doi.org/10.5194/hess-2019-305
Preprint. Discussion started: 10 July 2019


Hydrology and Earth System Sciences
Discussions

surface (upper side of the diagonal line in the matrices) against 24.7% for finer textures (lower side of the diagonal line in the matrices).

Figure 4 highlights that simulated soil evaporation decreases from fine to coarse textures, so that capillary retention, which is the main limiting factor to soil evaporation in ORCHIDEE, depends more strongly on soil moisture (higher for fine soils) than on intrinsic capillary forces (stronger for fine soils). We fail to see this behaviour in Figure 3, which is likely due to the greater impact of diverse climatic conditions and vegetation associated with every soil texture. This point-scale analysis also confirms the results of Figure 3 for the other variables, including the decrease of soil moisture with coarser soils and the greater impact of soil texture on runoff variables (surface runoff and drainage).

3.2. Sensitivity to different soil texture maps

Although ORCHIDEE exhibits a clear and physically-based response to soil texture at point-scale, the use of three different realistic soil texture maps (EXP2, EXP3 and EXP4) results in very similar terrestrial water budgets (Fig. 5). Whichever the hydrologic variable, the global mean differences induced by these three maps are smaller than the ones induced by different meteorological forcing (EXP1 vs EXP2), which are comparable to the uncertainty range between several observation-based estimates of the terrestrial water budget (Section 2.3). Compared to these estimates, it is also worth noting that ORCHIDEE simulates fairly well the mean partition between evapotranspiration and total runoff with any of the complex texture maps. In contrast, the use of spatially uniform soil texture maps (EXP6 to EXP9) induces major differences in surface runoff, drainage and soil moisture. The different water budgets resulting from these uniform maps are in agreement with the response of the model to soil texture (section 3.1). In particular, the uniform clay map (EXP9) induces high soil moisture and surface runoff, and low drainage, compared to the other uniform maps, while the uniform coarse map (Loamy Sand in EXP8, but Sand would give similar results based on Fig. 3) shows the opposite behavior. Eventually, using a uniform coarse or clay texture (EXP8 or EXP9) brings the simulated global mean evapotranspiration and runoff out of the observed range, contrarily to the uniform medium texture maps (EXP6, EXP7).

These extreme uniform maps are set aside to examine how soil texture maps impact the spatial distribution of the simulated fluxes. We focus on evapotranspiration (Fig. 6), since comparison is possible with a spatially-distributed observation-based product (GLEAM). At a grid cell scale, changing the soil texture map (Fig. 6a-c) results in weak changes in simulated evapotranspiration, which are statistically significant over less than 35% of the land surface, against 77% when switching the climate forcing (Fig. 6d). In agreement with the concave response of evapotranspiration to soil texture (section 3.1), the largest increases are found when switching from very coarse or very fine textures to medium ones. This explains the dominance of evapotranspiration increase in the example cases of Figures 6a-b, since the Zobler and uniform Loam maps have the largest areal fractions of Loam (Table 1). The area where evapotranspiration decreases in South-East Asia in Figure 6a (with Clay Loam in SoilGrids) probably results from the large variability of the flux response to soil texture in Figure 3.

https://doi.org/10.5194/hess-2019-305
Preprint. Discussion started: 10 July 2019

Although the other simulated hydrologic variables display a stronger sensitivity to soil texture maps, in agreement with section 3.1, it remains weak and predominantly insignificant in front of internal variability (Fig. 7, S3).

Consistently, the evapotranspiration biases are overall similar whichever the soil texture map (Fig. 6e-g, Fig S2), while climate forcing uncertainty is confirmed as a first order driving factor of the bias patterns (Fig. 6g-h). We find that the simulated evapotranspiration better matches GLEAM with CRU-NCEP in equatorial rain belts, and with GSWP3 in the mid-latitudes. In a few spots, however, the different soil maps can lead to strongly different evapotranspiration biases. In particular, the Zobler and Reynolds maps respectively produce a strong positive bias in Sudan and western India (Fig. 6f), and a strong negative bias in the eastern Amazon basin (Fig. 6g), further confirmed by an overestimation of simulated river discharge in this area (not shown). These biases are all related to the Clay texture, as discussed below.

4. Discussion and conclusions

Using the ORCHIDEE LSM and different soil texture maps, we found that the model shows a realistic sensitivity of surface runoff, drainage and soil moisture to soil texture compared to experimental and field studies (Rawls et al., 1993; Osman, 2013). These sensitivities lead to higher simulated evapotranspiration and lower total runoff for medium textures, which are discernable against other sources of variability when sorting the twelve USDA texture classes based on their median diameter. The three complex soil texture maps tested here, however, lead to similar water budgets at all scales, and the large uncertainties in observation-based products and climate forcing datasets make it impossible to conclude which map gives the best simulation.

These numerical results are specific to the ORCHIDEE model and the selected maps, but this model and these maps are representative examples of most state-of-the-art LSM applications (Vereecken et al., 2019), and comparable results were obtained with another LSM and other maps (De Lannoy et al., 2014). Besides, preliminary analyses of the LSM simulations conducted for the SP-MIP project (Gudmundsson & Cuntz, 2017) seem to confirm that varying soil parameters (resulting from different soil texture maps and different PTFs) have a small impact on long-term mean simulated evapotranspiration compared to other relevant uncertainties, including inter-model differences.

The weak sensitivity of the model to the three complex soil maps is probably largely explained by their spatial similarity, as supported by their large fraction of Loam (at least 44% in all the maps) and large overlap (29% between the three maps, and over 41% between each pair of maps, cf. Figure 8). This similarity primarily comes from their shared dependence on the FAO/UNESCO Soil Map, although weaker in SoilGrids. Another reason is the coarse spatial resolution at which soil texture is used in ORCHIDEE and most LSMs, since selecting the dominant soil texture in every grid cell (here 0.5°) statistically enhances medium textures. As the latter lead to higher evapotranspiration and smaller total runoff than more extreme textures (with larger percent of sand or clay particles), an important consequence, from a water budget point of view, is that dominant soil textures should favor excessive evapotranspiration and insufficient total runoff.

https://doi.org/10.5194/hess-2019-305
Preprint. Discussion started: 10 July 2019


Hydrology and Earth System Sciences
Discussions

Many alternative parameter upscaling methods were proposed to better preserve high resolution soil information, often based on averaging operators (usefully optimized to match coarse-scale observed streamflow in Samaniego et al., 2010), while Montzka et al. (2017) deduce upscaled parameters from theoretically upscaled hydraulic conductivity and diffusivity curves. More invasive approaches would consist in describing the effects of high resolution soil information directly in the model equations, as frequently done for the effect of K_s on infiltration owing to tractable statistical distributions (Vereecken et al., 2019). We lack similar developments for the full range of simulated water fluxes, apart from the partitioning of each grid cell into three soil columns with different soil textures, tested by de Rosnay et al. (2002) in ORCHIDEE but now abandoned. The texture maps themselves can also be questioned. When compared to the FAO soil order map (Fig. S4), SoilGrids tends to amplify the extent of sandy soils in Sahara and Saudi Arabia but ignores most sandy soils in Asia (e.g. Taklamakan desert). These shortcomings have a weak impact on simulated evapotranspiration, which is very low in these deserts, but larger biases can be attributed to the Clay class, although it covers small fractions of the globe. Of particular relevance is the distinction between: Vertisols, consisting of swelling clay (smectites) with low permeability, and mostly found in dry regions like Sudan, Deccan (India), or eastern Australia; Oxisols, which are found in humid Tropics, exhibit a large textural variability, and contain non-swelling clay (kaolinite) with much higher permeability than Vertisols. Using the Reynolds map, evapotranspiration is significantly underestimated over the basement rocks of eastern Amazonia, where Oxisols are assumed to belong to the Clay class. This led the ORCHIDEE development group to prefer the simplified Zobler map to conduct IPSL CMIP6 simulations. Yet, positive evapotranspiration biases occur where Vertisols are not mapped as Clay, as in Sudan and Deccan in the latter map.

More generally, the use of simple PTFs based on soil texture classes only is increasingly questioned. Firstly, they overlook the first-order influence of bulk density and soil structure, which require information on organic matter content (Smettem, 1987; Rahmati et al., 2018; Sun et al., 2018) and coarse fragments exceeding 2 mm, frequent in many soils (Brakensiek and Rawls, 1994; Valentin, 1994). Secondly, the simplifying assumption that soil texture is homogeneous vertically throughout the soil column should be revised. A particular attention should be paid on surface soil properties in areas prone to soil crusting (Valentin et al., 2008; Gal et al., 2017), which mainly include loamy soils (Rawls et al., 1990) and also arid and semi-arid soils (Valentin and Bresson, 1992), producing high total runoff (Yair, 1990; Casenave and Valentin, 1992; Karambiri et al., 2003; Bouvier et al., 2018). All these factors should be incorporated in PTFs and LSMs to improve the simulated hydrology.

Code availability

The version of the ORCHIDEE model used for this study is based on tag 2.0, freely available from http://forge.ipsl.jussieu.fr/orchidee/browser/tags/ORCHIDEE_2_0/ORCHIDEE/

https://doi.org/10.5194/hess-2019-305
Preprint. Discussion started: 10 July 2019

Small modifications were coded to read new maps of soil texture or soil parameters, and the corresponding code can be obtained upon request to first author.

Author contribution

ST, AD and CV designed the research. ST performed the simulations, analysed the data and prepared a draft of the manuscript. All authors contributed to interpreting results, discussing findings and improving the manuscript.

Competing interests

The authors declare that they have no conflict of interest.

Acknowledgments

The ORCHIDEE simulations were performed using the IDRIS computational facilities (Institut du Développement et des Ressources en Informatique Scientifique, CNRS, France). Some of them were designed by Lukas Gudmundsson and Matthias Cuntz for the SP-MIP project.

References

Al-Yaari, A., Ducharne, A., Cheruy, F., Crow, W. T. and Wigneron, J.-P.: Satellite-based soil moisture provides missing link between summertime precipitation and surface temperature biases in CMIP5 simulations over conterminous United States, Sci. Rep., 9(1), 1657, doi:10.1038/s41598-018-38309-5, 2019.

An, N., Tang, C.-S., Xu, S.-K., Gong, X.-P., Shi, B. and Inyang, H. I.: Effects of soil characteristics on moisture evaporation, Eng. Geol., 239, 126–135, doi:10.1016/j.enggeo.2018.03.028, 2018.

Batjes, N. H.: Harmonized soil property values for broad-scale modelling (WISE30sec) with estimates of global soil carbon stocks, Geoderma, 269, 61–68, doi:10.1016/j.geoderma.2016.01.034, 2016.

Bouvier, C., Bouchenaki, L. and Tramblay, Y.: Comparison of SCS and Green-Ampt Distributed Models for Flood Modelling in a Small Cultivated Catchment in Senegal, Geosciences, 8(4), 122, doi:10.3390/geosciences8040122, 2018.

Brakensiek, D. L. and Rawls, W. J.: Soil containing rock fragments: effects on infiltration, CATENA, 23(1), 99–110, doi:10.1016/0341-8162(94)90056-6, 1994.

Bughici, T. and Wallach, R.: Formation of soil–water repellency in olive orchards and its influence on infiltration pattern, Geoderma, 262, 1–11, doi:10.1016/j.geoderma.2015.08.002, 2016.

Carsel, R. F. and Parrish, R. S.: Developing joint probability distributions of soil water retention characteristics, Water Resour. Res., 24(5), 755–769, doi:10.1029/WR024i005p00755, 1988.

Casenave, A. and Valentin, C.: A runoff capability classification system based on surface features criteria in semi-arid areas of West Africa, J. Hydrol., 130(1), 231–249, doi:10.1016/0022-1694(92)90112-9, 1992.

Cheng, F.-Y. and Chen, Y.: Variations in soil moisture and their impact on land–air interactions during a 6-month drought period in Taiwan, Geosci. Lett., 5(1), 26, doi:10.1186/s40562-018-0125-8, 2018.

Clapp, R. B. and Hornberger, G. M.: Empirical equations for some soil hydraulic properties, Water Resour. Res., 14(4), 601–604, doi:10.1029/WR014i004p00601, 1978.

Compo, G. P., Whitaker, J. S., Sardeshmukh, P. D., Matsui, N., Allan, R. J., Yin, X., Gleason, B. E., Vose, R. S., Rutledge, G., Bessemoulin, P., Brönnimann, S., Brunet, M., Crouthamel, R. I., Grant, A. N., Groisman, P. Y., Jones, P. D., Kruk, M. C., Kruger, A. C., Marshall, G. J., Maugeri, M., Mok, H. Y., Nordli, Ø., Ross, T. F., Trigo, R. M., Wang, X. L., Woodruff, S. D. and Worley, S. J.: The Twentieth Century Reanalysis Project, Q. J. R. Meteorol. Soc., 137(654), 1–28, doi:10.1002/qj.776, 2011.

Cosby, B. J., Hornberger, G. M., Clapp, R. B. and Ginn, T. R.: A Statistical Exploration of the Relationships of Soil Moisture Characteristics to the Physical Properties of Soils, Water Resour. Res., 20(6), 682–690, doi:10.1029/WR020i006p00682, 1984.

De Lannoy, G. J. M., Koster, R. D., Reichle, R. H., Mahanama, S. P. P. and Liu, Q.: An updated treatment of soil texture and associated hydraulic properties in a global land modeling system, J. Adv. Model. Earth Syst., 6(4), 957–979, doi:10.1002/2014MS000330, 2014.

De Rosnay, P., Polcher, J., Bruen, M. and Laval, K.: Impact of a physically based soil water flow and soil-plant interaction representation for modeling large-scale land surface processes, J. Geophys. Res. Atmospheres, 107(D11), ACL 3-1-ACL 3-19, doi:10.1029/2001JD000634, 2002.

Dong, J. and Ochsner, T. E.: Soil Texture Often Exerts a Stronger Influence Than Precipitation on Mesoscale Soil Moisture Patterns, Water Resour. Res., 54(3), 2199–2211, doi:10.1002/2017WR021692, 2018.

D'Orgeval, T., Polcher, J. and Rosnay, P. de: Sensitivity of the West African hydrological cycle in ORCHIDEE to infiltration processes, Hydrol. Earth Syst. Sci., 12(6), 1387–1401, doi:https://doi.org/10.5194/hess-12-1387-2008, 2008.

Ducharne, A., Ghattas, J., Maignan, F., Ottlé, C., Vuichard, N., Guimberteau, M., Krinner, G., Polcher, J., Tafasca, S., Bastrikov, V., Brender, P., Cheruy, F., Guénet, B., Mizuochi, H., Peylin, P., Tootchi, A. and Wang, F.: Soil water processes in the ORCHIDEE-2.0 land surface model: state of the art for CMIP6, Geosci. Model Dev., in prep.

Ducharne, A. and Laval, K.: Influence of the Realistic Description of Soil Water-Holding Capacity on the Global Water Cycle in a GCM, J. Clim., 13(24), 4393–4413, doi:10.1175/1520-0442(2000)013<4393:IOTRDO>2.0.CO;2, 2000.

Eswaran, H., Reich, P. and Padmanabhan, E.: World soil resources: Opportunities and challenges, in World Soil Resources and Food Security, pp. 29–51, CRC Press., 2012.

Eyring, V., Bony, S., Meehl, G. A., Senior, C. A., Stevens, B., Stouffer, R. J. and Taylor, K. E.: Overview of the Coupled Model Intercomparison Project Phase 6 (CMIP6) experimental design and organization, Geosci. Model Dev., 9(5), 1937–1958, doi:10.5194/gmd-9-1937-2016, 2016.

FAO and UNESCO: FAO-UNESCO Soil Map of the World, 1971-1981.

Gal, L., Grippa, M., Hiernaux, P., Pons, L. and Kergoat, L.: The paradoxical evolution of runoff in the pastoral Sahel: analysis of the hydrological changes over the Agoufou watershed (Mali) using the KINEROS-2 model, Hydrol. Earth Syst. Sci., 21(9), 4591–4613, doi:https://doi.org/10.5194/hess-21-4591-2017, 2017.

Guimberteau, M., Ducharne, A., Ciais, P., Boisier, J.-P., Peng, S., De Weirdt, M. and Verbeeck, H.: Testing conceptual and physically based soil hydrology schemes against observations for the Amazon Basin, Geosci. Model Dev., 7, 1115–1136, doi:10.5194/gmd-7-1115-2014, 2014.

Guimberteau, M., Ciais, P., Ducharne, A., Boisier, J. P., Dutra Aguiar, A. P., Biemans, H., De Deurwaerder, H., Galbraith, D., Kruijt, B., Langerwisch, F., Poveda, G., Rammig, A., Rodriguez, D. A., Tejada, G., Thonicke, K., Von Randow, C., Von Randow, R. C., Zhang, K. and Verbeeck, H.: Impacts of future deforestation and climate change on the hydrology of the Amazon Basin : a multi-model analysis with a new set of land-cover change scenarios, Hydrol. EARTH Syst. Sci., 21(3), 1455–1475, doi:http://dx.doi.org/10.5194/hess-21-1455-2017, 2017.

Gundmundsson, L. and Cuntz, M.: Soil Parameter Model Intercomparison Project (SP-MIP): Assessing the influence of soil parameters on the variability of Land Surface Models, [online] Available from: https://www.gewexevents.org/wp-content/uploads/GLASS2017_SP-MIP_Protocol.pdf (Accessed 4 April 2019), 2017.

Guo, Z., Dirmeyer, P. A., Hu, Z.-Z., Gao, X. and Zhao, M.: Evaluation of the Second Global Soil Wetness Project soil moisture simulations: 2. Sensitivity to external meteorological forcing, J. Geophys. Res. Atmospheres, 111(D22), doi:10.1029/2006JD007845, 2006.

Haddeland, I., Clark, D. B., Franssen, W., Ludwig, F., Voß, F., Arnell, N. W., Bertrand, N., Best, M., Folwell, S., Gerten, D., Gomes, S., Gosling, S. N., Hagemann, S., Hanasaki, N., Harding, R., Heinke, J., Kabat, P., Koirala, S., Oki, T., Polcher, J.,

https://doi.org/10.5194/hess-2019-305
Preprint. Discussion started: 10 July 2019

Stacke, T., Viterbo, P., Weedon, G. P. and Yeh, P.: Multimodel Estimate of the Global Terrestrial Water Balance: Setup and First Results, J. Hydrometeorol., 12(5), 869–884, doi:10.1175/2011JHM1324.1, 2011.

Hengl, T., Jesus, J. M. de, MacMillan, R. A., Batjes, N. H., Heuvelink, G. B. M., Ribeiro, E., Samuel-Rosa, A., Kempen, B., Leenaars, J. G. B., Walsh, M. G. and Gonzalez, M. R.: SoilGrids1km — Global Soil Information Based on Automated Mapping, PLOS ONE, 9(8), e105992, doi:10.1371/journal.pone.0105992, 2014.

Jung, M., Reichstein, M., Ciais, P., Seneviratne, S. I., Sheffield, J., Goulden, M. L., Bonan, G., Cescatti, A., Chen, J., de Jeu, R., Dolman, A. J., Eugster, W., Gerten, D., Gianelle, D., Gobron, N., Heinke, J., Kimball, J., Law, B. E., Montagnani, L., Mu, Q., Mueller, B., Oleson, K., Papale, D., Richardson, A. D., Roupsard, O., Running, S., Tomelleri, E., Viovy, N., Weber, U., Williams, C., Wood, E., Zaehle, S. and Zhang, K.: Recent decline in the global land evapotranspiration trend due to limited moisture supply, Nature, 467(7318), 951–954, doi:10.1038/nature09396, 2010.

Kalnay, E., Kanamitsu, M., Kistler, R., Collins, W., Deaven, D., Gandin, L., Iredell, M., Saha, S., White, G., Woollen, J., Zhu, Y., Chelliah, M., Ebisuzaki, W., Higgins, W., Janowiak, J., Mo, K. C., Ropelewski, C., Wang, J., Leetmaa, A., Reynolds, R., Jenne, R. and Joseph, D.: The NCEP/NCAR 40-Year Reanalysis Project, Bull. Am. Meteorol. Soc., 77(3), 437–472, doi:10.1175/1520-0477(1996)077<0437:TNYRP>2.0.CO;2, 1996.

Karambiri, H., Ribolzi, O., Delhoume, J. P., Ducloux, J., Coudrain□Ribstein, A. and Casenave, A.: Importance of soil surface characteristics on water erosion in a small grazed Sahelian catchment, Hydrol. Process., 17(8), 1495–1507, doi:10.1002/hyp.1195, 2003.

Kishné, A. S., Yimam, Y. T., Morgan, C. L. S. and Dornblaser, B. C.: Evaluation and improvement of the default soil hydraulic parameters for the Noah Land Surface Model, Geoderma, 285, 247–259, doi:10.1016/j.geoderma.2016.09.022, 2017.

Krinner, G., Viovy, N., Noblet-Ducoudré, N. de, Ogée, J., Polcher, J., Friedlingstein, P., Ciais, P., Sitch, S. and Prentice, I. C.: A dynamic global vegetation model for studies of the coupled atmosphere-biosphere system, Glob. Biogeochem. Cycles, 19(1), doi:10.1029/2003GB002199, 2005.

Lehmann, P., Merlin, O., Gentine, P. and Or, D.: Soil Texture Effects on Surface Resistance to Bare-Soil Evaporation, Geophys. Res. Lett., 45(19), 10,398-10,405, doi:10.1029/2018GL078803, 2018.

Li, J., Chen, F., Zhang, G., Barlage, M., Gan, Y., Xin, Y. and Wang, C.: Impacts of Land Cover and Soil Texture Uncertainty on Land Model Simulations Over the Central Tibetan Plateau, J. Adv. Model. Earth Syst., 10(9), 2121–2146, doi:10.1029/2018MS001377, 2018.

Lipiec, J., Kuś, J., Słowińska-Jurkiewicz, A. and Nosalewicz, A.: Soil porosity and water infiltration as influenced by tillage methods, Soil Tillage Res., 89(2), 210–220, doi:10.1016/j.still.2005.07.012, 2006.

Livneh, B., Kumar, R. and Samaniego, L.: Influence of soil textural properties on hydrologic fluxes in the Mississippi river basin, Hydrol. Process., 29(21), 4638–4655, doi:10.1002/hyp.10601, 2015.

Looy, K. V., Bouma, J., Herbst, M., Koestel, J., Minasny, B., Mishra, U., Montzka, C., Nemes, A., Pachepsky, Y. A., Padarian, J., Schaap, M. G., Tóth, B., Verhoef, A., Vanderborght, J., Ploeg, M. J. van der, Weihermüller, L., Zacharias, S., Zhang, Y. and Vereecken, H.: Pedotransfer Functions in Earth System Science: Challenges and Perspectives, Rev. Geophys., 55(4), 1199–1256, doi:10.1002/2017RG000581, 2017.

Martens, B., Miralles, D. G., Lievens, H., Schalie, R. van der, Jeu, R. A. M. de, Fernández-Prieto, D., Beck, H. E., Dorigo, W. A. and Verhoest, N. E. C.: GLEAM v3: satellite-based land evaporation and root-zone soil moisture, Geosci. Model Dev., 10(5), 1903–1925, doi:https://doi.org/10.5194/gmd-10-1903-2017, 2017.

Milly, P. C. D. and Dunne, K. A.: Sensitivity of the Global Water Cycle to the Water-Holding Capacity of Land, J. Clim., 7(4), 506–526, doi:10.1175/1520-0442(1994)007<0506:SOTGWC>2.0.CO;2, 1994.

Montzka, C., Herbst, M., Weihermüller, L., Verhoef, A. and Vereecken, H.: A global data set of soil hydraulic properties and sub-grid variability of soil water retention and hydraulic conductivity curves, Earth Syst. Sci. Data, 9(2), 529–543, doi:https://doi.org/10.5194/essd-9-529-2017, 2017.

Mostovoy, G. V. and Anantharaj, V. G.: Observed and Simulated Soil Moisture Variability over the Lower Mississippi Delta Region, J. Hydrometeorol., 9(6), 1125–1150, doi:10.1175/2008JHM999.1, 2008.

Mualem, Y.: A new model for predicting the hydraulic conductivity of unsaturated porous media, Water Resour. Res., 12(3), 513–522, doi:10.1029/WR012i003p00513, 1976.

Nachtergaele, F. O., Velthuizen, H. van, Verelst, L., Batjes, N. H., Dijkshoorn, J. A., Engelen, V. W. P. van, Fischer, G., Jones, A., Montanarela, L., Petri, M., Prieler, S., Shi, X., Teixeira, E. and Wiberg, D.: The Harmonized World Soil Database, 2010.

Osman, K. T.: Soils: Principles, Properties and Management, Springer Netherlands. [online] Available from: https://www.springer.com/gp/book/9789400756625 (Accessed 22 May 2019), 2013.

Priestley, C. H. B. and Taylor, R. J.: On the Assessment of Surface Heat Flux and Evaporation Using Large-Scale Parameters, Mon. Weather Rev., 100(2), 81–92, doi:10.1175/1520-0493(1972)100<0081:OTAOSH>2.3.CO;2, 1972.

Rahmati, M., Weihermüller, L., Vanderborght, J., Pachepsky, Y. A., Mao, L., Sadeghi, S. H., Moosavi, N., Kheirfam, H., Montzka, C., Looy, K. V., Toth, B., Hazbavi, Z., Yamani, W. A., Albalasmeh, A. A., Alghzawi, M. Z., Angulo-Jaramillo, R., Antonino, A. C. D., Arampatzis, G., Armindo, R. A., Asadi, H., Bamutaze, Y., Batlle-Aguilar, J., Béchet, B., Becker, F., Blöschl, G., Bohne, K., Braud, I., Castellano, C., Cerdà, A., Chalhoub, M., Cichota, R., Císlerová, M., Clothier, B., Coquet, Y., Cornelis, W., Corradini, C., Coutinho, A. P., Oliveira, M. B. de, Macedo, J. R. de, Durães, M. F., Emami, H., Eskandari, I., Farajnia, A., Flammini, A., Fodor, N., Gharaibeh, M., Ghavimipanah, M. H., Ghezzehei, T. A., Giertz, S., Hatzigiannakis, E. G., Horn, R., Jiménez, J. J., Jacques, D., Keesstra, S. D., Kelishadi, H., Kiani-Harchegani, M., Kouselou, M., Kumar Jha, M., Lassabatere, L., Li, X., Liebig, M. A., Lichner, L., López, M. V., Machiwal, D., Mallants, D., Mallmann, M. S., Marques, O., De, J. D., Marshall, M. R., Mertens, J., Meunier, F., Mohammadi, M. H., Mohanty, B. P., Pulido-Moncada, M., Montenegro, S., Morbidelli, R., Moret-Fernández, D., Moosavi, A. A., Mosaddeghi, M. R., Mousavi, S. B., Mozaffari, H., Nabiollahi, K., Neyshabouri, M. R., Ottoni, M. V., Filho, O., Benedicto, T., Pahlavan-Rad, M. R., Panagopoulos, A., Peth, S., Peyneau, P.-E., Picciafuoco, T., Poesen, J., Pulido, M., Reinert, D. J., Reinsch, S., Rezaei, M., Roberts, F. P., Robinson, D., Rodrigo-Comino, J., et al.: Development and analysis of the Soil Water Infiltration Global database, Earth Syst. Sci. Data, 10(3), 1237–1263, doi:https://doi.org/10.5194/essd-10-1237-2018, 2018.

Rawls, W. J., Brakensiek, D. L., Simanton, J. R. and Kohl, K. D.: Development of a crust factor for a Green-Ampt model, Trans. ASAE, 33(4), 1224–1228, 1990.

Rawls, W. J., Ahuja, L. R., Brakensiek, D. L. and Shirmohammadi, A.: Infiltration and soil water movement, in: Handbook of Hydrology, New York. Available from: https://ci.nii.ac.jp/naid/10018251877/ (Accessed 23 May 2019), 1993.

Remaud, M., Chevallier, F., Cozic, A., Lin, X. and Bousquet, P.: On the impact of recent developments of the LMDz atmospheric general circulation model on the simulation of CO2 transport, Geosci. Model Dev., 11(11), 4489–4513, doi:10.5194/gmd-11-4489-2018, 2018.

Reynolds, C. A., Jackson, T. J. and Rawls, W. J.: Estimating soil water-holding capacities by linking the Food and Agriculture Organization Soil map of the world with global pedon databases and continuous pedotransfer functions, Water Resour. Res., 36(12), 3653–3662, doi:10.1029/2000WR900130, 2000.

Rodell, M., Beaudoing, H. K., L'Ecuyer, T. S., Olson, W. S., Famiglietti, J. S., Houser, P. R., Adler, R., Bosilovich, M. G., Clayson, C. A., Chambers, D., Clark, E., Fetzer, E. J., Gao, X., Gu, G., Hilburn, K., Huffman, G. J., Lettenmaier, D. P., Liu, W. T., Robertson, F. R., Schlosser, C. A., Sheffield, J. and Wood, E. F.: The Observed State of the Water Cycle in the Early Twenty-First Century, J. Clim., 28(21), 8289–8318, doi:10.1175/JCLI-D-14-00555.1, 2015.

Schaap, M. G., Leij, F. J. and van Genuchten, M. T.: rosetta: a computer program for estimating soil hydraulic parameters with hierarchical pedotransfer functions, J. Hydrol., 251(3), 163–176, doi:10.1016/S0022-1694(01)00466-8, 2001.

Smettem, K. R. J.: Characterization of water entry into a soil with a contrasting textural class: spatial variability of infiltration parameters and influence of macroporosity, Soil Sci., 144(3), 167–174, 1987.

Song, R., Chu, G., Ye, J., Bai, L., Zhang, R. and Yang, J.: Effects of surface soil mixed with sand on water infiltration and evaporation in laboratory, Editor. Off. Trans. Chin. Soc. Agric. Eng., 26(1), 109–114, 2010.

Sterling, S. M., Ducharne, A. and Polcher, J.: The impact of global land-cover change on the terrestrial water cycle, Nat. Clim. Change, 3(4), 385–390, doi:10.1038/nclimate1690, 2013.

Sun, D., Yang, H., Guan, D., Yang, M., Wu, J., Yuan, F., Jin, C., Wang, A. and Zhang, Y.: The effects of land use change on soil infiltration capacity in China: A meta-analysis, Sci. Total Environ., 626, 1394–1401, doi:10.1016/j.scitotenv.2018.01.104, 2018.

USDA Soil Survey Staff and Bureau of Plant Industry, Soils and agricultural Engineering: Soil survey manual, Agricultural Research Administration, U.S. Dept. of Agriculture, Washington, D.C., 1951.

https://doi.org/10.5194/hess-2019-305
Preprint. Discussion started: 10 July 2019

425 Valentin, C.: Surface sealing as affected by various rock fragment covers in West Africa, CATENA, 23(1), 87–97, doi:10.1016/0341-8162(94)90055-8, 1994.

Valentin, C. and Bresson, L.-M.: Morphology, genesis and classification of surface crusts in loamy and sandy soils, Geoderma, 55(3), 225–245, doi:10.1016/0016-7061(92)90085-L, 1992.

Valentin, C., Agus, F., Alamban, R., Boosaner, A., Bricquet, J. P., Chaplot, V., de Guzman, T., de Rouw, A., Janeau, J. L.,
430 Orange, D., Phachomphonh, K., Do Duy Phai, Podwojewski, P., Ribolzi, O., Silvera, N., Subagyono, K., Thiébaux, J. P., Tran Duc Toan and Vadari, T.: Runoff and sediment losses from 27 upland catchments in Southeast Asia: Impact of rapid land use changes and conservation practices, Agric. Ecosyst. Environ., 128(4), 225–238, doi:10.1016/j.agee.2008.06.004, 2008.

Van den Hurk, B., Kim, H., Krinner, G., Seneviratne, S. I., Derksen, C., Oki, T., Douville, H., Colin, J., Ducharne, A.,
435 Cheruy, F., Viovy, N., Puma, M. J., Wada, Y., Li, W., Jia, B., Alessandri, A., Lawrence, D. M., Weedon, G. P., Ellis, R., Hagemann, S., Mao, J., Flanner, M. G., Zampieri, M., Materia, S., Law, R. M. and Sheffield, J.: LS3MIP (v1.0) contribution to CMIP6: the Land Surface, Snow and Soil moisture Model Intercomparison Project – aims, setup and expected outcome, Geosci Model Dev, 9(8), 2809–2832, doi:10.5194/gmd-9-2809-2016, 2016.

Van Genuchten, M.: A Closed-form Equation for Predicting the Hydraulic Conductivity of Unsaturated Soils 1, Soil Sci.
440 Soc. Am. J., 44(5), 892–898, doi:10.2136/sssaj1980.03615995004400050002x, 1980.

Vereecken, H., Pachepsky, Y., Bogena, H. and Montzka, C.: Upscaling Issues in Ecohydrological Observations, in Observation and Measurement of Ecohydrological Processes, edited by X. Li and H. Vereecken, pp. 435–454, Springer Berlin Heidelberg, Berlin, Heidelberg., 2019.

Wang, F., Cheruy, F. and Dufresne, J.-L.: The improvement of soil thermodynamics and its effects on land surface
445 meteorology in the IPSL climate model, Geosci. Model Dev., 9(1), 363–381, doi:https://doi.org/10.5194/gmd-9-363-2016, 2016.

Wang, T., Istanbulluoglu, E., Lenters, J. and Scott, D.: On the role of groundwater and soil texture in the regional water balance: An investigation of the Nebraska Sand Hills, USA, Water Resour. Res., 45(10), W10413, doi:10.1029/2009WR007733, 2009.

450 Wei, Y., Liu, S., Huntzinger, D. N., Michalak, A. M., Viovy, N., Post, W. M., Schwalm, C. R., Schaefer, K., Jacobson, A. R., Lu, C., Tian, H., Ricciuto, D. M., Cook, R. B., Mao, J. and Shi, X.: The North American carbon program multi-scale synthesis and terrestrial model intercomparison project – Part 2: Environmental driver data, Geosci. Model Dev. Discuss., 7, 2875–2893, 2014.

Xia, Y., Ek, M. B., Wu, Y., Ford, T. and Quiring, S. M.: Comparison of NLDAS-2 Simulated and NASMD Observed Daily
455 Soil Moisture. Part II: Impact of Soil Texture Classification and Vegetation Type Mismatches, J. Hydrometeorol., 16(5), 1981–2000, doi:10.1175/JHM-D-14-0097.1, 2015.

Yair, A.: Runoff generation in a sandy area—the nizzana sands, Western Negev, Israel, Earth Surf. Process. Landf., 15(7), 597–609, doi:10.1002/esp.3290150703, 1990.

Yin, Z., Ottle, C., Ciais, P., Guimberteau, M., Wang, X., Zhu, D., Maignan, F., Peng, S., Piao, S., Polcher, J., Zhou, F. and
460 Kim, H.: Evaluation of ORCHIDEE-MICT-simulated soil moisture over China and impacts of different atmospheric forcing data, Hydrol. Earth Syst. Sci., 22(10), 5463–5484, doi:10.5194/hess-22-5463-2018, 2018.

Zhao, F., Veldkamp, T. I. E., Frieler, K., Schewe, J., Ostberg, S., Willner, S., Schauberger, B., Gosling, S. N., Schmied, H. M., Portmann, F. T., Leng, G., Huang, M., Liu, X., Tang, Q., Hanasaki, N., Biemans, H., Gerten, D., Satoh, Y., Pokhrel, Y., Stacke, T., Ciais, P., Chang, J., Ducharne, A., Guimberteau, M., Wada, Y., Kim, H. and Yamazaki, D.: The critical role of
465 the routing scheme in simulating peak river discharge in global hydrological models, Environ. Res. Lett., 12(7), 075003, doi:10.1088/1748-9326/aa7250, 2017.

Zheng, H. and Yang, Z.-L.: Effects of soil-type datasets on regional terrestrial water cycle simulations under different climatic regimes, J. Geophys. Res. Atmospheres, 121(24), 14387–14402, doi:10.1002/2016JD025187, 2016.

Zobler, L.: A world soil hydrology file for global climate modeling. National Aeronautics and Space Administration,
470 Technical memorandum 87802, 1986.

https://doi.org/10.5194/hess-2019-305
Preprint. Discussion started: 10 July 2019

Hydrology and Earth System Sciences
Discussions
Open Access
EGU

Tables and Figures

475

Table 1. Summary of the experiments used in this study. Texture distribution displays the percentage of each soil texture in the used soil map.* Indicates the experiments used in the SP-MIP.

Experiment	Soil map	Climate Forcing	PTF	Text.Distrib
EXP1	Reynolds	CRU-NCEP	Carsel & Parrish (1988)	
EXP2	Reynolds	GSWP3	Carsel & Parrish (1988)	
EXP3*	Zobler	GSWP3	Carsel & Parrish (1988)	
EXP4*	SoilGrids	GSWP3	Carsel & Parrish (1988)	
EXP5*	SoilGrids	GSWP3	Schaap et al. (2001)	
EXP6*	Loam	GSWP3	Schaap et al. (2001)	
EXP7*	Silt	GSWP3	Schaap et al. (2001)	
EXP8*	Loamy Sand	GSWP3	Schaap et al. (2001)	
EXP9*	Clay	GSWP3	Schaap et al. (2001)	

480 **Table 2. Percent sand, silt and clay contents of the geometric centroids of the 12 USDA soil texture classes. *dm*: the computed median diameter.**

Texture class	Label	% Clay	% Silt	% Sand	*dm* (µm)
Clay	C	62.9	17.5	19.5	1.6
Silty Clay	SiC	46.7	46.7	6.7	5.4
Silty Clay Loam	SiCL	33.8	56.3	10.0	15.9
Clay Loam	CL	33.8	33.8	32.5	25.1
Silt	Si	5.3	87.3	7.3	26.6
Silt Loam	SiL	13.4	65.2	21.4	29.0
Loam	L	18.7	40.2	41.0	39.3
Sandy Clay	SaC	41.7	6.7	51.7	112.9
Sandy Clay Loam	SaCL	27.1	12.9	59.9	373.3
Sandy Loam	SaL	10.4	25.1	64.6	490.7
Loamy Sand	LSa	5.8	12.5	81.7	806.1
Sand	Sa	3.3	5.0	91.7	936.4

485

https://doi.org/10.5194/hess-2019-305
Preprint. Discussion started: 10 July 2019

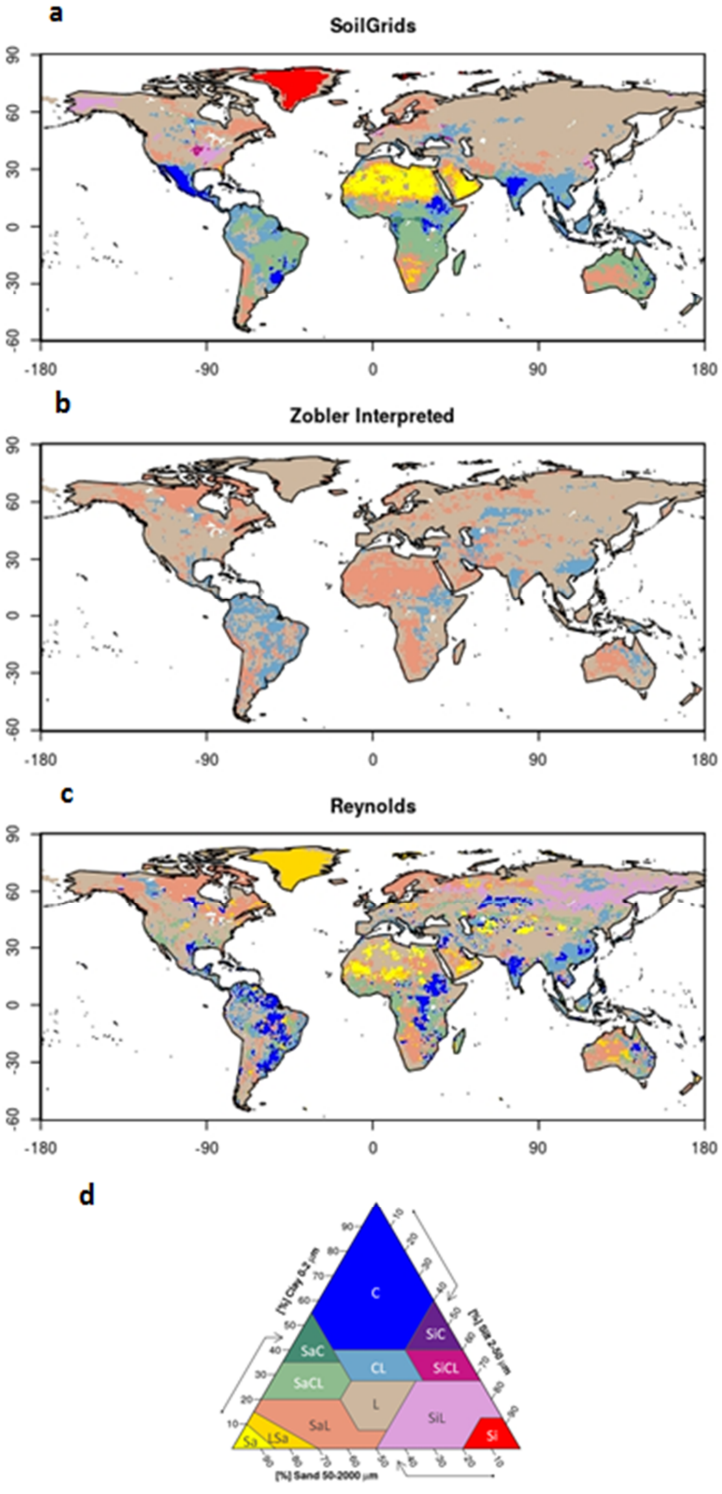

490

https://doi.org/10.5194/hess-2019-305
Preprint. Discussion started: 10 July 2019

Hydrology and Earth System Sciences
Discussions
Open Access
EGU

Figure 1. (a-c) Global maps of soil texture classes used in this study. (d) Soil texture triangle of the 12 textural classes as defined by the USDA. For texture labels see Table 2.

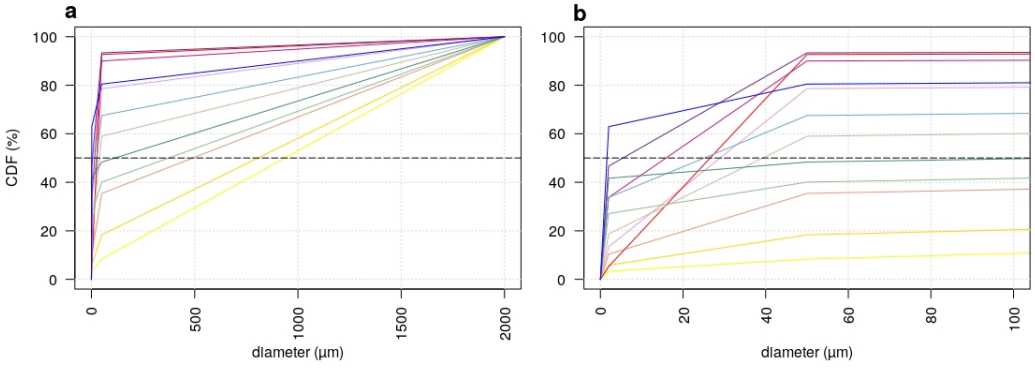

Figure 2. (a) Cumulative grain size distribution curves of the 12 USDA soil texture classes and (b) zoom over diameter interval [0,100 µm]. The dashed line defines the 50% cumulative value.

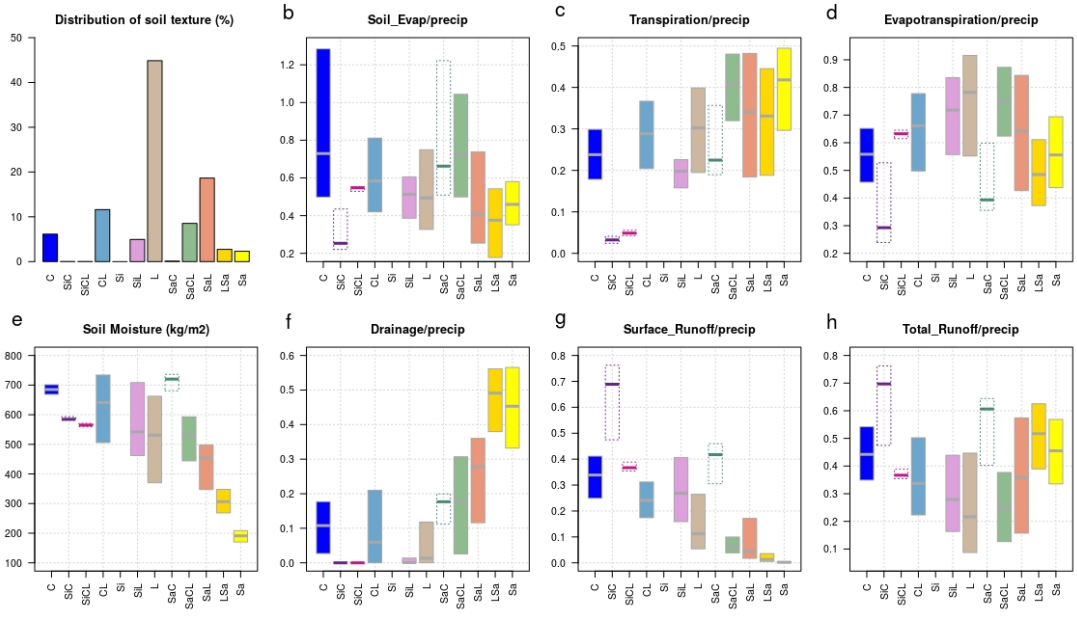

Figure 3. Variability of simulated variables of EXP2 over the land surface excluding Antarctica and Greenland, over the period 1980-2010, within each soil texture class. Soil texture classes are sorted from the finest to the coarsest based on dm (from left to right). See Figure 1 for color codes. Note that the Silt class is absent from Reynolds map. Dashed boxes correspond to texture classes covering less than 0.2% of the land area. Water fluxes are expressed as percent precipitation. Soil moisture is averaged over areas with similar annual precipitation (between 1 and 2 mm/d), to remove impact of precipitation variation. Transpiration and soil evaporation fluxes are averaged over vegetated and bare soil fractions of the grid cells respectively.

https://doi.org/10.5194/hess-2019-305
Preprint. Discussion started: 10 July 2019

Hydrology and Earth System Sciences
Discussions

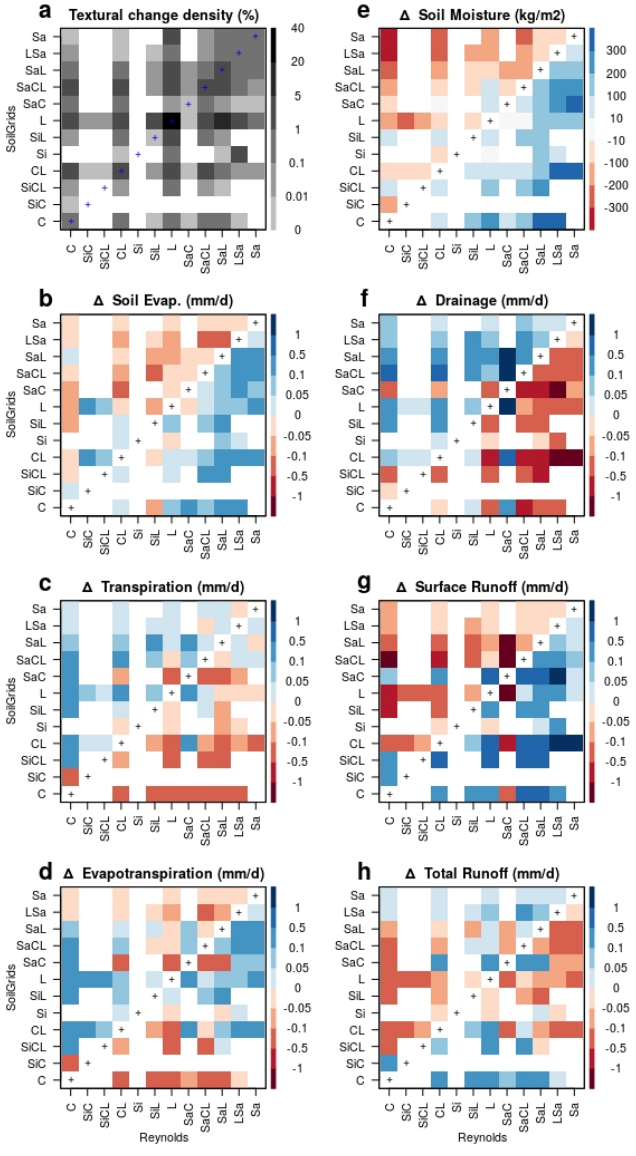

Figure 4. Change in mean simulated variables over the globe land surface excluding Antarctica, averaged over the period 1980-2010, caused by changing the soil texture map from Reynolds to SoilGrids (EXP2 to EXP4). Soil texture classes are sorted from the finest (clay) to the coarsest (sand), in the x and y axis. The first plot illustrates the percentage of each textural change.

https://doi.org/10.5194/hess-2019-305
Preprint. Discussion started: 10 July 2019

Hydrology and Earth System Sciences
Discussions
Open Access
EGU

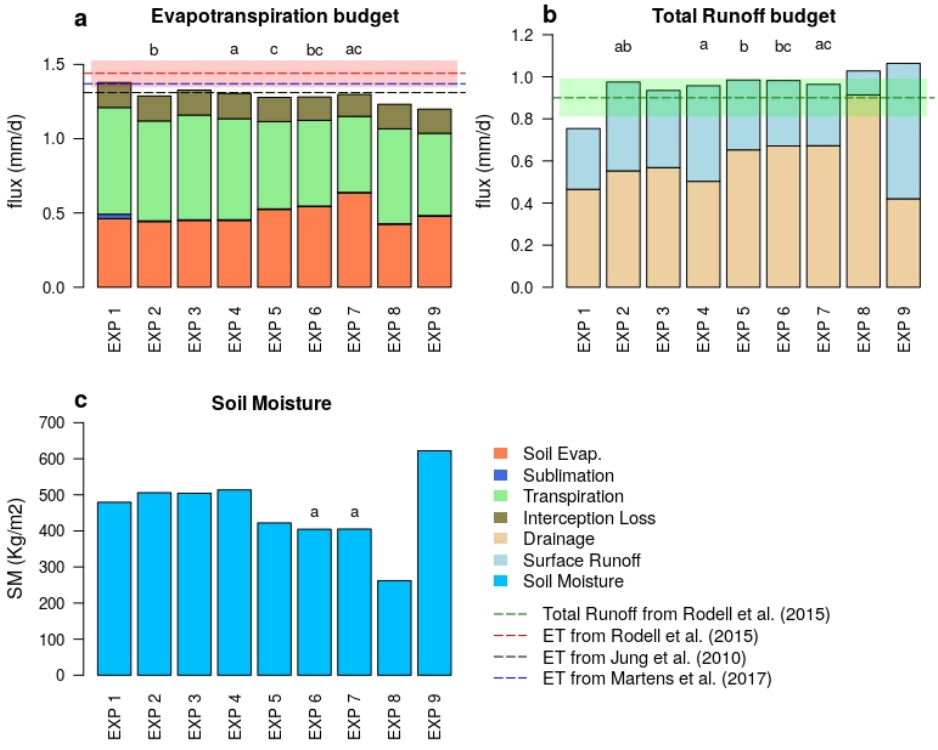

Figure 5. Terrestrial water budget components for the nine simulations of Table 1, on average over 1980-2010 and over all land areas but Antarctica: (a) Evapotranspiration budget; (b) Total runoff budget; (c) Soil moisture. Letters above bars describe statistical significance: the mean difference between bars with the same letter is not statistically significant based on Student's t-test (with a p-value of 5%). Red and green semi-transparent bands show the uncertainty range in the estimates of Rodell et al. (2015), for evapotranspiration and total runoff respectively. The estimated values of evapotranspiration and total runoff used for evaluation are described in section 2.3.

https://doi.org/10.5194/hess-2019-305
Preprint. Discussion started: 10 July 2019

Hydrology and Earth System Sciences
Discussions
Open Access
EGU

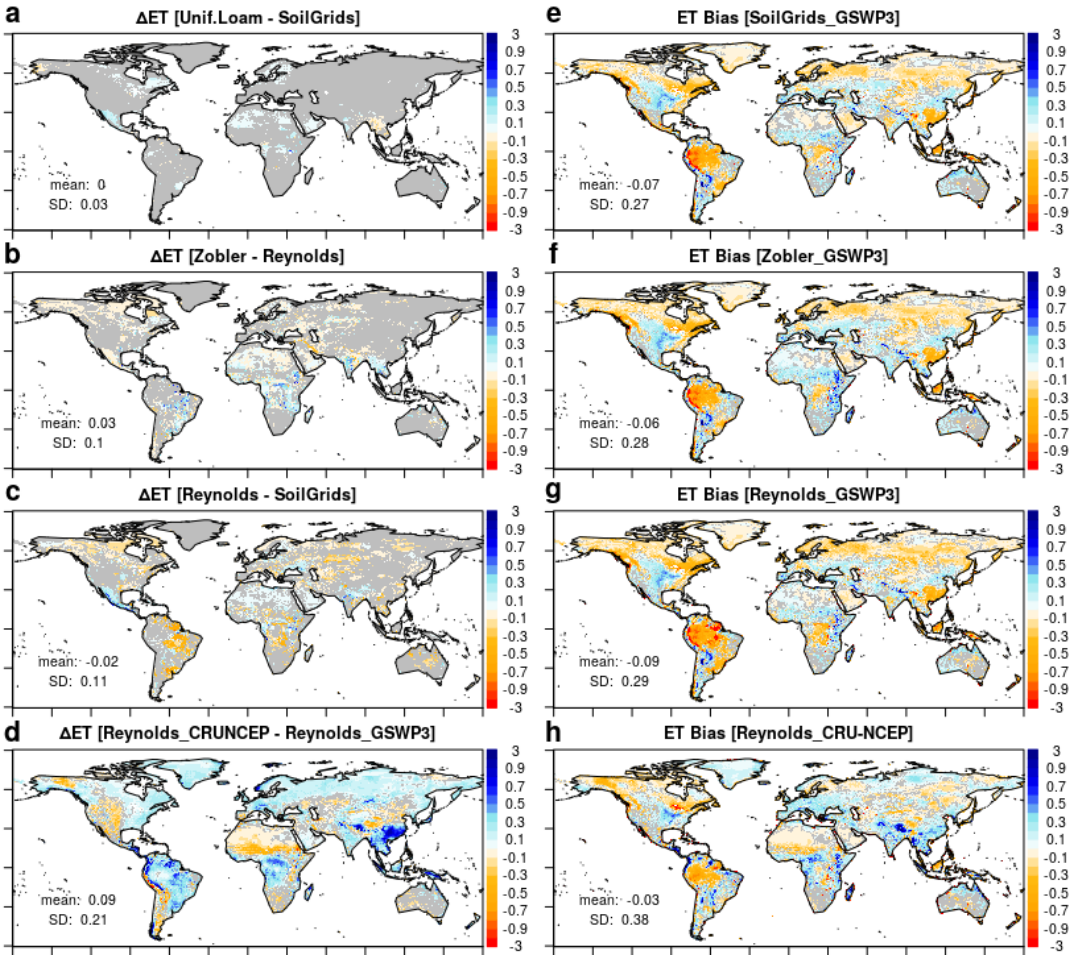

Figure 6. Spatial distribution of simulated annual mean evapotranspiration: (left) differences between selected pairs of simulations (a: EXP6-EXP5, b: EXP3- EXP2, c: EXP2-EXP4, d: EXP1-EXP2); (right) biases with respect to GLEAM product (e: EXP4, f: EXP3, g: EXP2, h: EXP1). Grey color indicates that the difference is not statistically significant based on Student's t-test (with a p-value of 5%). The printed means and standard deviation correspond to the full land area excluding Antarctica. Maps of GLEAM and simulated evapotranspiration of the 9 experiments are presented in Supplementary Figure S2.

https://doi.org/10.5194/hess-2019-305
Preprint. Discussion started: 10 July 2019

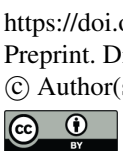

Hydrology and Earth System Sciences
Discussions

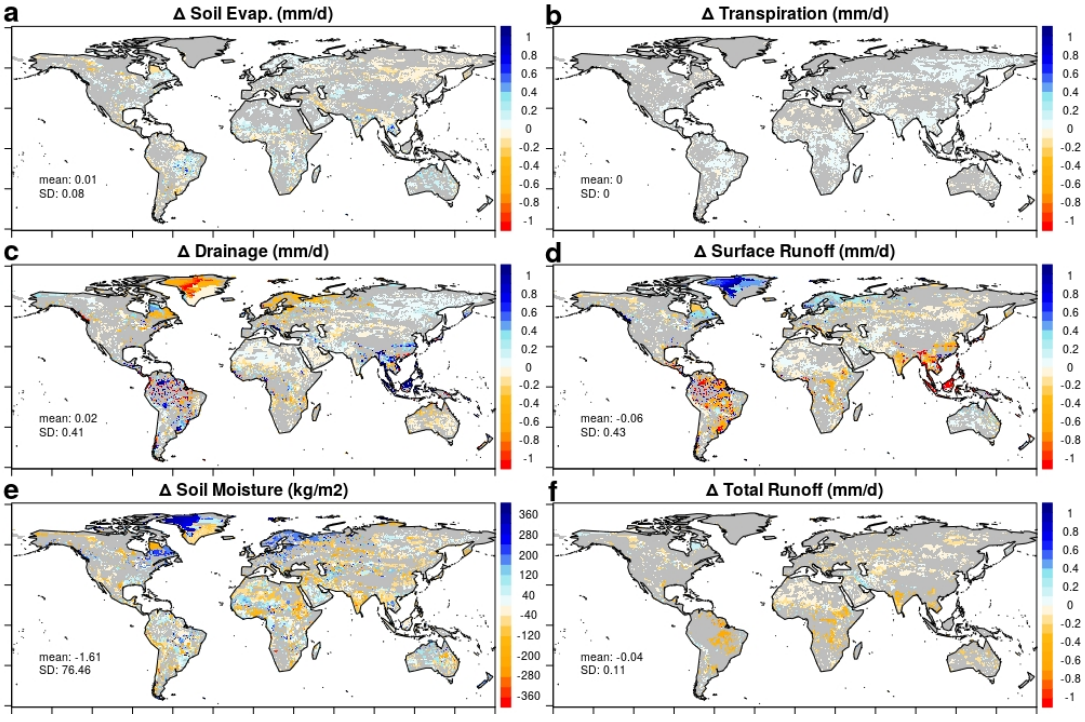

Figure 7. Difference in simulated variables when Reynolds map is replaced by a Zobler map (EXP3 – EXP2), averaged over the period 1980-2010. The corresponding difference for evapotranspiration is shown in Fig. 6b. Grey color indicates that the difference is not statistically significant based on Student's t-test (with a p-value of 5%). Mean and standard deviation are averaged over the globe excluding Antarctica.

(a)

	SoilGrids	Reynolds	Zobler
SoilGrids	100		
Reynolds	41.2	100	
Zobler	46.0	52.0	100
Unif. Loam	48.5	43.9	64.3
Unif. Silt	3.3	0	0
Unif. Loamy Sand	2.1	6	0
Unif. Clay	2.7	5.8	0

(b)

	SoilGrids	Reynolds	Zobler
SoilGrids	1		
Reynolds	0.27	1	
Zobler	0.34	0.43	1

Figure 8. Indicators of similarity between the different soil texture maps: (a) Percent overlap between the texture maps. (b) Correlation coefficients between maps of soil particles diameter (soil texture maps were converted to soil particles median diameter maps using Table 2).